

High-energy γ -ray Emission from Microquasars: LS 5039 and LS I +61 303

V. Bosch-Ramon^{*} and J. M. Paredes

Departament d'Astronomia i Meteorologia, Universitat de Barcelona, Av. Diagonal 647,
E-08028 Barcelona, Spain

Abstract The possible associations between the microquasars LS 5039 and LS I +61 303 and the EGRET sources 3EG J1824–1514 and 3EG J0241+6103 suggest that microquasars could also be sources of high-energy γ -rays. In this work, we present a detailed numerical inverse Compton (IC) model, based on a microquasar scenario, that reproduces the high-energy γ -ray spectra and variability observed by EGRET for the mentioned sources. Our model considers a population of relativistic electrons entrained in a cylindrical inhomogeneous jet that interact through IC scattering with both the radiation and the magnetic fields.

Key words: X-rays: binaries — Stars: LS 5039, LS I +61 303 — gamma-rays: observations — gamma-rays: theory

1 INTRODUCTION

Microquasars are a selected class of X-ray binaries that produce relativistic radio jets (Mirabel & Rodríguez 1999, Fender 2004). The origin of the jets is related to the matter accreted by the compact object, a neutron star or a black hole, from the companion star. These systems behave as scaled-down versions of quasars and active galactic nuclei. The population of microquasars is still a very reduced one, with about sixteen known objects up to now (Ribó 2002). Due to the presence in these systems of both a relativistic jet with a population of highly relativistic leptons and strong radiation fields, microquasars are promising γ -ray emitter candidates through IC interaction (for synchrotron self Compton (SSC) models, see, i.e. Atoyan & Aharonian 1999; for external Compton (EC) models, see, i.e. Kaufman Bernadó et al. 2002), although these sources could emit at such energy ranges by other means (i.e. see the hadronic model of Romero et al. 2003). We are interested on determining whether a microquasar jet emitting by IC scattering can reproduce the EGRET data of the two sources associated to microquasars: 3EG J1824–1514/LS 5039 and 3EG J0241+6103/LS I +61 303. Our numerical model considers a population of relativistic electrons entrained in a cylindrical inhomogeneous jet interacting with both the radiation and the magnetic fields, accounting for the synchrotron, the EC and the SSC electron energy losses.

^{*} E-mail: vbosch@am.ub.es

2 LS 5039 AND LS I +61 303

LS 5039 is a High Mass X-ray binary system (HMXB) located at 2.9 kpc from Earth (Ribó et al. 2002). The stellar companion is a bright ($V \sim 11$) star of ON6.5 V((f)) spectral type, the compact object seems to be a neutron star, the orbital period of the system is $P = 4.4267 \pm 0.0005$ days, the eccentricity, $e = 0.48 \pm 0.06$, and the semi-major axis of the orbit $a = 2.6 \times 10^{12}$ cm (McSwain et al. 2004). The microquasar nature of LS 5039 was clearly established when non-thermal radiation produced in a mildly relativistic jet was detected, being also proposed as the counterpart of the unidentified γ -ray source 3EG J1824–1514 (Paredes et al. 2000).

LS I +61 303 is another HMXB whose optical counterpart is a bright ($V \sim 10.8$) star of B0 V spectral type (Paredes & Figueras 1986), presenting an equatorial disk (Be star) and harbouring likely a neutron star as a compact object (Hutchings & Crampton 1981). This source is at a distance of about 2 kpc. The more accurate value for the orbital period is $P = 26.4960 \pm 0.0028$ days (Gregory 2002), the eccentricity is $e \sim 0.7$ (Casares et al. 2005), and the orbital semi-major axis is about $a = 5 \times 10^{12}$ cm. This source presents variability at different timescales, from radio to γ -rays (see, i.e., Taylor & Gregory 1982, Paredes & Figueras 1986, Goldoni & Mereghetti 1995, Tavani et al. 1998, Massi 2004). The microquasar nature of LS I +61 303 was established when a mildly relativistic jet structure was detected through VLBI observations of this source (Massi et al. 2001, 2004), although this object had already been proposed to be the counterpart of the γ -ray source 2CG 135+01/3EG J0241+6103 (Gregory & Taylor 1978, Kniffen et al. 1997).

3 MODELLING THE γ -RAY EMISSION FROM MICROQUASARS

In this model, we assume that the leptons of the jet dominate the radiative processes related to the γ -ray production. The relativistic population of electrons, already accelerated and flowing away into the jet, is exposed to external photons as well as to the synchrotron photons emitted by the electrons, since we take into account the magnetic field in our model. The γ -ray emitting region, the γ -jet, is assumed to be closer to the compact object than the observed radio jets. This γ -jet is supposed to be short enough to be considered cylindrical. The magnetic field (B_γ) has been taken to be constant, as an average along the jet. The energy losses of the relativistic leptonic plasma at the γ -jet are mainly due to synchrotron emission, SSC scattering, and EC scattering. Due to the importance of the losses, the electron energy distribution density along the γ -jet model varies significantly, thus the γ -jet is studied by splitting it into cylindrical transverse cuts or slices.

Regarding IC interaction, we have used the cross-section of Blumenthal & Gould (1970), $\sigma(x, \epsilon_0, \gamma_e)$, which takes into account the Thomson and the Klein-Nishina regimes of interaction; ϵ_0 is the seed photon energy, γ_e is the scattering electron Lorentz factor, and x is actually a function which depends on both of the former quantities and on the scattered photon energy (ϵ). The electron distribution is assumed to be initially a power law ($N(\gamma_e) \propto E^{-p}$, where E is the electron energy), which evolves under the conditions imposed by the magnetic and the radiation fields. Thus, the electron distribution function of a certain slice ($N(\gamma_e, z)$) depends on both the distance to the compact object (z) and γ_e . The components of the total seed photon radiation field ($U(\epsilon_0, z)$) are any present external radiation field ($U_{\text{ext}}(\epsilon_0, z)$) and the synchrotron radiation field produced by the jet's relativistic electrons, all of them in the jet's reference frame (for the external photon fields, see Dermer & Schlickeiser 2002). It must be noted that, since LS 5039 and LS I +61 303 are not strong X-ray emitters, we will assume that the most important source of seed photons is the companion star, neglecting at the present stage the disk and corona contributions (see Bosch-Ramon et al. 2005). The formulae that represent $U(\epsilon_0, z)$ and its components (a black-body stellar photon field and a synchrotron photon field) are well described in the work of Bosch-Ramon & Paredes (2004).

The free parameters of the model are B_γ and the maximum electron Lorentz factor at the slice closest to the compact object (γ_{e0}^{\max}). The leptonic kinetic luminosity or leptonic jet power (L_{ke}) is set free also, and it is scaled with the observed luminosity, in order to reproduce the observations. The jet radius, although it is not well constrained, has been fixed to several electron Larmor radii ($\sim 10^7$ cm), and the electron power-law index of the injected distribution has been deduced from radio observations (for LS 5039, see Martí et al. 1998; for LS I +61 303, see Ray et al. 1997). The luminosity per energy unit in the reference frame of the jet (L_ϵ) is presented in Eq. 1. The photon flux per energy unit or spectral photon distribution in the reference frame of the observer ($I'_{\epsilon'}$) is shown in Eq. 2. The magnitudes with ($'$) are in the observer reference frame.

$$L_\epsilon = \epsilon \sum_{z_{\min}}^{z_{\max}} V_{\text{slice}}(z) \int_{\epsilon_0^{\min}(z)}^{\epsilon_0^{\max}(z)} \int_{\gamma_e^{\min}(z)}^{\gamma_e^{\max}(z)} \frac{U(\epsilon_0, z)}{\epsilon_0} N(\gamma_e, z) \frac{d\sigma(x, \epsilon_0, \gamma_e)}{d\epsilon} d\gamma d\epsilon_0 \quad (1)$$

$$I'_{\epsilon'} = \frac{\delta^{2+p}}{4\pi D^2 \epsilon'} L_{\epsilon'} \quad (2)$$

where δ is the Doppler factor of the jet, D is the distance from the microquasar to the observer, and $V_{\text{slice}}(z)$ is the volume of the slice at a distance z from the compact object. For further details of the model, see Bosch-Ramon & Paredes (2004, 2004b).

4 RESULTS AND CONCLUSIONS

We have applied our model to both LS 5039 and LS I +61 303 in order to reproduce the spectra observed by EGRET. In Table 1, the known parameter values as well as the adopted values for the free parameters are presented. The computed spectral photon distributions are shown in the Figs. 1 and 2 for LS 5039 and LS I +61 303, respectively. The results show that these microquasars can produce high-energy γ -rays through IC interaction between a relativistic leptonic population, entrained in an inhomogeneous cylindrical jet, and the external and synchrotron photon fields.

Table 1 Parameter values for LS 5039 and LS I +61 303

Parameter	Adopted values for LS 5039 / LS I +61 303
Jet Lorentz factor (Γ_{jet})	1.02 / 1.25
Angle between the jet and the observer line of sight (θ)	30°
Jet velocity (v_{jet})	$0.2c$ / $0.6c$
Orbital semi-major axis (a)	2.6×10^{12} / 5×10^{12} cm
Orbital eccentricity (e)	0.5 / 0.7
Distance to the observer (D)	2.9 / 2 kpc
Star total luminosity (L_{star})	1.2×10^{39} / 2×10^{38} erg s $^{-1}$
Photon flux at the EGRET band ($I_{>100 \text{ MeV}}$)	3.3×10^{-7} / 8×10^{-7} photon cm $^{-2}$ s $^{-1}$
Photon index at the EGRET band (Γ)	~ 2.2
Jet radius (R_γ)	10^7 cm
Injected electron power-law index (p)	2 / 1.7
Free parameter	Adopted values for LS 5039 / LS I +61 303
Magnetic field (B_γ)	1–10 G
Leptonic jet power (L_{ke})	10^{35} – 3×10^{35} / 10^{36} – 3×10^{36} erg s $^{-1}$
Maximum electron Lorentz factor (γ_{e0}^{\max})	10^5

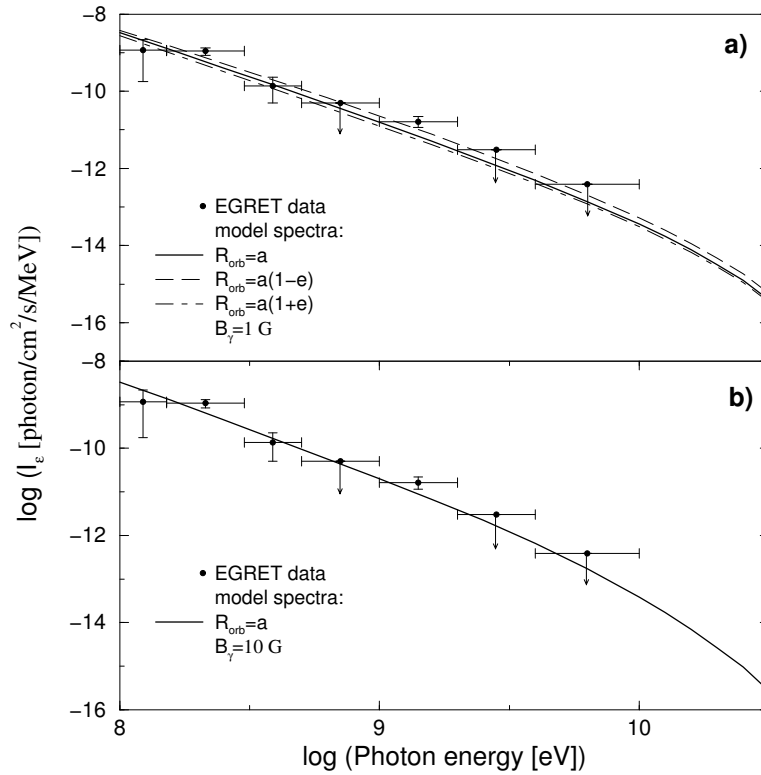


Fig. 1 Computed IC spectral photon distribution above 100 MeV for LS 5039 using the physical parameter values presented in Table 1. The EGRET data points are also shown. The upper limits on undetected EGRET points are plotted with arrows. Only stellar radiation density changes due to the orbital eccentricity have been taken into account. **a)** A magnetic field of 1 G has been adopted. Also, the IC spectral photon distribution for both the apastron and the periastron passage are shown. **b)** A magnetic field of 10 G has been adopted.

Our model can reproduce EGRET data with reasonable parameter values, and variability is naturally expected from stellar radiation and accretion changes due to orbital eccentricity (precession can introduce also variability, see *Massi et al. 2004*). Since, at the present stage, no clear varying accretion influence has been detected in LS 5039 at lower energies, we have not introduced it to compute the presented spectral photon distributions (see Fig. 1), but only the eccentric orbit effects on the stellar radiation density. However, since orbital eccentricity is clearly affecting radio (*Taylor & Gregory 1982*) and X-ray emission (*Goldoni & Mereghetti 1995*) in the case of LS I +61 303, we have taken into account it to calculate its emission at γ -rays. The magnetic field can control the loss of energy of the electrons by SSC losses. Therefore, with two magnetic field strengths: 1 and 10 G, the emission turns from being dominated by EC effect to be dominated by the SSC effect. It is shown in Fig. 1, where emission is not affected by the eccentricity of the orbit when the magnetic field is high, since changes in the stellar photon density do not affect the spectrum in the SSC dominant regime (accretion changes are not included in the calculations). It is worth noting also that in the case of LS I +61 303, where accretion changes are taken into account, they are far more important than the stellar photon density variations, implying almost the same effects on the spectrum variability for both cases, the EC and the SSC ones.

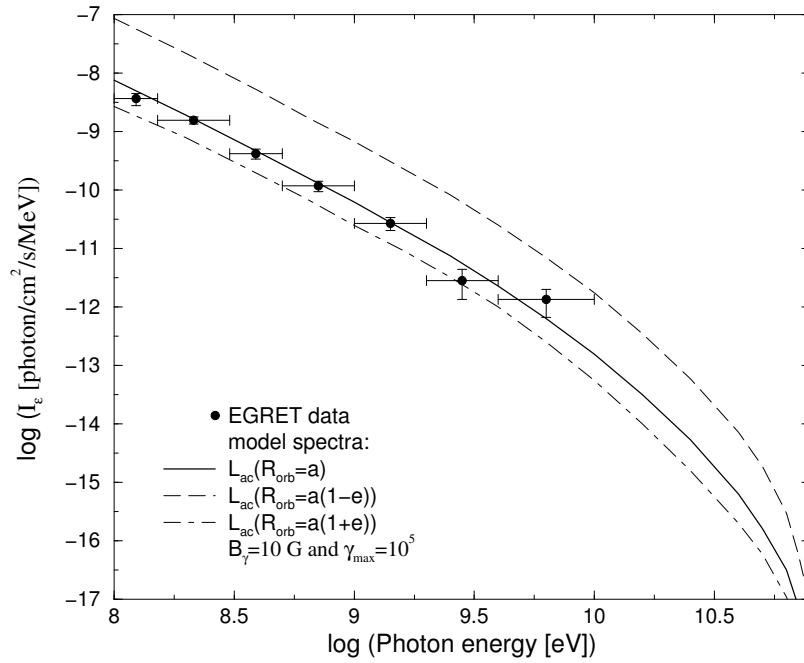


Fig. 2 Computed spectral photon distribution above 100 MeV for LS I +61 303 plotted with the EGRET data points. We have used the physical parameter values presented in Table 1. Unlike in Fig. 1, the spectral shape and the variability are the same for both $B_\gamma=1$ and 10 G. Thus there is only one plot. There are plotted the computed I'_γ for different orbital radii: a (solid line), the distance at the periastron passage ($a(1-e)$, dashed line), and the distance at the apastron passage ($a(1+e)$, dotted line). Now, accretion changes due to orbital eccentricity have been included in calculations.

These results strengthen the idea that microquasars are γ -ray emitters, being LS 5039 and LS I +61 303 likely counterparts of the two EGRET sources 3EG J1824–1514 and 3EG J0241+6103 respectively. However, further observations with the new generation of γ -ray instruments (i.e. AGILE, GLAST, HESS, MAGIC, etc...) are mandatory in order to get enough angular resolution, flux and temporal sensitivity and energy range width to determine properly the association microquasars/EGRET sources and to better constrain the current models of emission.

Acknowledgements V.B-R. and J.M.P. acknowledge partial support by DGI of the Ministerio de Ciencia y Tecnología (Spain) under grant AYA-2001-3092, as well as additional support from the European Regional Development Fund (ERDF/FEDER). During this work, V.B-R has been supported by the DGI of the Ministerio de Ciencia y Tecnología (Spain) under the fellowship FP-2001-2699.

References

- Atoyan, A. M. & Aharonian, F. A. 1999, MNRAS, 302, 253
 Blumenthal, G. R. & Gould, R. J. 1970, RMP, 42, 237
 Bosch-Ramon, V., Romero, G. E., & Paredes, J. M. 2005, A&A, 429, 267
 Bosch-Ramon, V. & Paredes, J. M. 2004, A&A, 417, 1075
 Bosch-Ramon, V. & Paredes, J. M. 2004b, A&A, 425, 1069

- Casares, J., Ribas, I., Paredes, J. M., et al. 2005, MNRAS, in press
- Dermer, C. D. & Schlickeiser, R. 2002, ApJ, 575, 667
- Fender, R., to appear in 2004, Compact Stellar X-Ray Sources, eds. W.H.G. Lewin and M. van der Klis, Cambridge University Press
- Goldoni, P. & Mereghetti, S. 1995, A&A, 299, 751
- Gregory, P. C. & Taylor, A. R. 1978, Nature, 272, 704
- Gregory, P. C. 2002, ApJ, 575, 427
- Hutchings, J. B. & Crampton, D. 1981, PASP, 93, 486
- Kaufman Bernadó, M. M., Romero, G. E., & Mirabel, I. F. 2002, A&A, 385, L10–L13
- Kniffen, D. A., Alberts, W. C. K., Bertsch, D. L. et al. 1997, ApJ, 486, 126
- Martí, J., Paredes, J. M., & Ribó, M. 1998, A&A, 338, L71
- Massi, M., Ribó, M., Paredes, J. M., Peracaula, M., & Estalella, R. 2001, A&A, 376, 217
- Massi, M. 2004, A&A, 422, 267
- Massi, M., Ribó, M., Paredes J. M., et al 2004, A&A, 414, L1
- McSwain, M. V., Gies D. R., Huang W., et al. 2004, ApJ, 600, 927
- Mirabel, I. F. & Rodríguez, L. F. 1999, ARA&A, 37, 409
- Paredes, J. M. & Figueras, F. 1986, A&A, 154, L30
- Paredes, J. M., Martí, J., Ribó, M., & Massi, M. 2000, Science, 288, 2340
- Ray, P. S., Foster, R. S., Waltman, E. B., Tavani, M., & Ghigo, F. D. 1997, ApJ, 491, 381
- Ribó, M. 2002, PhD Thesis, Universitat de Barcelona
- Ribó, M., Paredes, J. M., & Romero, G. E., et al. 2002, A&A, 384, 954
- Romero, G. E., Torres, D. F., Kaufman Bernadó, M. M., & Mirabel, I. F. 2003, A&A, 410, L1
- Tavani, M., Kniffen, D., Mattox, J. R., Paredes, J. M., & Foster, R. 1998, ApJ, 497, L89
- Taylor, A. R. & Gregory, P. C. 1982, ApJ, 255, 210